Transport physics dependence of Bohm speed in presheath-sheath transition

Li, Yuzhi
Srinivasan, Bhuvana
Zhang, Yanzeng
Tang, Xianzhu

To be published in: Physics of Plasmas

DOI to publisher's version: 10.1063/5.0110379

Transport physics dependence of Bohm speed in presheath-sheath transition

Yuzhi Li,[1] Bhuvana Srinivasan,[1] Yanzeng Zhang,[2] and Xian-Zhu Tang[2]
[1)]*Kevin T. Crofton Department of Aerospace and Ocean Engineering, Virginia Tech, Blacksburg, Virginia 24060, USA*
[2)]*Theoretical Division, Los Alamos National Laboratory, Los Alamos, New Mexico 87545, USA*

(Dated: 10 October 2022)

The ion exit flow speed at the sheath entrance is constrained by the Bohm criterion, which is used as a boundary condition for simulations that do not resolve the sheath region. Traditional Bohm criterion analysis invokes the equation of state and thus ignores transport physics in the sheath transition problem. An expression for the Bohm speed away from the asymptotic limit is derived from a set of anisotropic plasma transport equations. The thermal force, collisional temperature isotropization, and heat flux enter into the evaluation of the Bohm speed. By comparison with kinetic simulation results, this expression is shown to be accurate in the presheath-sheath transition region rather than a single point at the sheath entrance over a broad range of collisionality.

I. INTRODUCTION

When a plasma is in contact with solid boundaries, due to the greater mobility of electrons, a sheath forms next to the wall[1]. A negative potential arises at the wall compared with the bulk plasma to equalize the electron and ion fluxes. The negative potential at the boundary is shielded out over a few Debye lengths λ_D and the bulk plasma remains quasineutral. The solid boundary acts as a particle and heat sink. It introduces large gradients of temperature, density and potential in the sheath, making the plasma near the boundary deviate strongly from thermodynamic equilibrium. Most fluid and gyrokinetic codes do not resolve the sheath region. Instead, a sheath boundary condition is imposed at the simulation boundary to exclude the non-neutral sheath region from the simulation.[2–4]. Usually, the so-called sheath boundary condition, which constrains the ion exit flow speed (e.g., Ref.[5–7]), sheath potential drop (e.g., Ref.[8–10]), and the outgoing ion and electron energy fluxes (e.g., Ref.[11,12]), is deduced from either analytical theory or non-neutral plasma simulations using both kinetic and fluid models, for example, see Ref.[5–9,11–16].

The plasma-sheath transition problem was first investigated in early works of Langmuir[8], where the quasineutral plasma and the non-neutral sheath are separated by a sheath entrance. The presheath electric field can accelerate the ions to a finite speed at the sheath entrance. Assuming the plasma consists of monoenergetic ions and Boltzmann electrons, Bohm showed that the ion exit flow speed has a lower bound at the sheath entrance: $u_i \geq \sqrt{T_e/m_i}$, also known as the Bohm criterion[5] and the lower bound of the ion exit flow is the Bohm speed u_{Bohm}. Here, T_e is the electron temperature and m_i is the ion mass. This provides a criterion for the sheath to form, which has a fundamental role in understanding plasma-material interaction. The original Bohm criterion analysis assumes cold ions. In many applications, the ion temperature is usually comparable to the electron temperature. Several fluid models have been developed to solve the sheath transition problem accounting for finite ion temperature, such as the isothermal[13] and the adiabatic fluid models[14]. For different assumptions of the ions, the Bohm criterion can be generalized using adiabatic indices of electrons and ions, γ_e and γ_i, and the Bohm speed in these limits equals to the ion sound speed $c_s(\gamma_e,\gamma_i)$[9],

$$u_i \geq u_{Bohm} = c_s(\gamma_e,\gamma_i) \equiv \sqrt{(\gamma_e T_e + \gamma_i T_i)/m_i}, \qquad (1)$$

with T_i being the ion temperature. Due to high thermal conductivity, electrons are assumed to be isothermal, so $\gamma_e = 1$. For different plasma fluid models, ions can be assumed to be cold, isothermal, or adiabatic, leading to different Bohm speeds at the sheath entrance. These Bohm speeds are commonly used in plasma simulation codes as the sheath boundary conditions. For instance, the isothermal sound speed $c_s(1,1) = \sqrt{(T_e+T_i)/m_i}$ is used in SOLPS[2].

Much of transport physics has not been considered in the fluid sheath theory, despite the role of plasma transport near the sheath entrance and in the sheath can be significant and the plasma sheath transition problem is kinetic in nature. As a result, a number of key assumptions made in the classical sheath theory are not adequate. From the observation of recent first-principle kinetic simulations[17], the particle loss to the wall can introduce a significant temperature gradient for both species, implying that neither electrons nor ions are isothermal. Also, the electrons are far from isotropic in that the temperature normal to the wall is significantly lower than the temperature parallel to the wall due to the decompressional cooling in the flow direction. The temperature anisotropy excites the Weibel instability and introduces a self-generated magnetic field parallel to the wall.

When collisional transport is considered in the sheath transition problem[7], the findings contradict the conventional practice of equating the Bohm speed u_{Bohm} to the sound speed $c_s(\gamma_e,\gamma_i)$. For a plasma with low collisionality, $\gamma_{e,i}$ will be large since the plasma is neither isotropic nor isothermal, so is c_s. As collisionality increases, the Coulomb collisions can isotropize the plasma temperature, and $\gamma_{e,i}$ as well as c_s will decrease. In sharp contrast, the Bohm speed increases with the collisionality as seen from the first-principle kinetic simulation results. To resolve this, Tang and Guo[7] pointed to the missing transport physics, i.e., the heat flux terms, that would be the leading order in a boundary layer analysis. From their

analysis, the Bohm criterion becomes

$$u_i \geq \sqrt{(3\beta T_{e\|} + 3T_{i\|})/m_i}, \tag{2}$$

where $\|$ refers to the direction parallel to the external magnetic field that is normal to the wall, and β is the heat flux factor

$$\beta \equiv \frac{1 - \dfrac{\partial}{\partial\phi}\left(\dfrac{q_n^i}{e n_i^{se} u_{i\|}^{se}}\right)}{1 + \dfrac{\partial}{\partial\phi}\left(\dfrac{q_n^e}{e n_e^{se} u_{e\|}^{se}}\right)}. \tag{3}$$

Here, q_n is the parallel heat flux, n the density, $u_\|$ the parallel flow, and ϕ the electrostatic potential. The superscript se implies the sheath entrance. For a collisional plasma and collisionless sheath, a truncated bi-Maxwellian model[10] is used to calculate the electron heat flux q_n^e analytically, where $q_n^e \approx 2e\Gamma_{e\|}$ with $\Gamma_{e\|} = n_e u_{e\|}$ being the electron parallel flux. Usually, the ion heat flux q_n^i is much smaller than the electron heat flux q_n^e, so it is usually neglected in the analysis. Coincidentally, the resulting Bohm speed is $\sqrt{(T_{e\|} + 3T_{i\|})/m_i}$, not because of the isothermal electron assumption, but due to the electron heat flux[7] that results in the coefficient of T_e being 1.

The sheath entrance is defined in the asymptotic limit $\lambda_D/L \to 0$ with λ_D the Debye length and L the system size for a two-scale analysis[6]. In this limit, the Bohm criterion applies only at this sharp sheath entrance, where the ion exit flow speed reaches the Bohm speed u_{Bohm}. However, in applications away from this limit, there is a transition region between the plasma and the non-neutral sheath, where quasineutrality is weakly violated. The definition of the sheath entrance away from $\lambda_D/L \to 0$ becomes ambiguous since now it is extended to a region. Matched asymptotic expansion[18,19] of a plasma with cold ions and hot electrons indicate the existence of a transition layer and the ion flow reaches the Bohm speed $\sqrt{T_e/m_i}$ inside this transition layer.

This work resolves the discrepancies between kinetic simulations of sheath and fluid sheath theory, and applies the Bohm criterion to real plasmas away from the asymptotic limits. The sheath transition problem is investigated by elucidating the critical roles of various transport physics. The paper is organized as follows. In section II, an expression for the Bohm speed is derived considering various transport physics, including heat flux, collisional isotropization, and thermal force. The sheath profile away from the asymptotic limit $\lambda_D \to 0$ is shown in Section III by conducting kinetic simulations using the VPIC code[20]. In Section IV, away from the asymptotic limit, the sheath entrance is extended to a sheath transition region where the Bohm criterion can be applied. The accuracy of the Bohm speed model over a broad range of collisionality and the importance of transport physics in evaluating the Bohm speed is demonstrated in Section V.

II. PLASMA TRANSPORT MODEL AND DERIVATION OF THE BOHM SPEED

A. Key ingredients of the plasma transport model for presheath-sheath transition

To tackle the plasma-sheath transition problem, one needs to solve Poisson's equation coupled with a set of plasma transport equations. Around the sheath transition region, where the quasineutrality remains a good approximation $n_e \approx Zn_i$, Poisson's equation can be linearized by expanding the net charge $\rho = e(n_i - n_e)$ around 0,

$$\frac{\partial^2\phi}{\partial x^2} \approx 4\pi e \left(\frac{\partial n_e}{\partial\phi} - \frac{\partial n_i}{\partial\phi}\right)\Big|_{\phi=\phi^{se}} \phi. \tag{4}$$

where the potential at the sheath entrance is set zero $\phi^{se} = 0$. A non-oscillatory (pre)sheath requires

$$\left(\frac{\partial n_e}{\partial\phi} - \frac{\partial n_i}{\partial\phi}\right)\Big|_{\phi=\phi^{se}} \geq 0. \tag{5}$$

This is the Bohm criterion, also known as sheath criterion in the literature.

The Bohm speed can be obtained by plugging different plasma models into Eq. 5. Traditionally, the plasma transport equations can be closed with assumptions such as cold, isothermal or adiabatic ions and isothermal electrons, leading to expression in Eq. 1. However, from previous kinetic studies of the plasma sheath, it is known that the transport near the sheath entrance is highly anisotropic[17]. Moreover, the plasma collisionality has a huge influence on the Bohm speed[7]. Note though the influence of ion-neutral collision on the Bohm speed in an interesting question[21], here we are interested in fully ionized plasmas where only the Coulomb collision is considered. The collisionality of the system can be characterized by a sheath Knudsen number: $K_n^{sh} \equiv \lambda_{mfp}/\lambda_D$[7], the ratio of the Coulomb collisional mean free path to the Debye length at the sheath entrance. This work studies the regime of $K_n^{sh} > 1$ or $K_n^{sh} \gg 1$, in which the plasma transport is important. Due to the anisotropic nature of the plasma sheath-transition problem, the mean free path is defined as $\lambda_{mfp} \equiv v_{th,e}/\nu_{ei}$ with $v_{th,e} = \sqrt{T_{ex}/m_e}$ the electron thermal speed and ν_{ei} the anisotropic electron-ion collision frequency given by Eq. 9. For a collisional system with $K_n^{sh} > 1$ or $K_n^{sh} \gg 1$, the force due to collisions may play a role in momentum transport. The collisional force can be considered as the sum of two kinds of forces[22], the friction force due to the relative fluid velocity between different species and the thermal force due to the temperature gradient. In a steady state sheath, the electron and ion charge fluxes equalize, so the friction force is negligible. However, electrons are not isothermal and the electron temperature gradient may give rise to the thermal force R_T. The collisional heating in energy transport consists of temperature relaxation between different species, relaxation of anisotropy, and Ohmic heating. The Ohmic heating is trivial due to the vanishing net current in steady-state and the thermal equilibration rate is slow due to the large ion-electron mass ratio. Whereas, the collisional isotropization for

each species plays an important role in the energy transport due to the strong temperature anisotropy in the (pre)sheath. A set of anisotropic plasma transport equations in the steady state can be written as[23–26]

$$\frac{\partial n_e u_{ex}}{\partial x} = 0; \quad \frac{\partial n_i u_{ix}}{\partial x} = 0, \tag{6a}$$

$$\frac{\partial n_e T_{ex}}{\partial x} = e n_e \frac{\partial \phi}{\partial x} - \alpha n_e \frac{dT_{ex}}{dx}, \tag{6b}$$

$$n_i m_i u_{ix} \frac{\partial u_{ix}}{\partial x} + \frac{\partial n_i T_{ix}}{\partial x} = -Z e n_i \frac{\partial \phi}{\partial x} + \alpha n_e \frac{dT_{ex}}{dx}, \tag{6c}$$

$$n_e u_{ex} \frac{\partial T_{ex}}{\partial x} + 2 n_e T_{ex} \frac{\partial u_{ex}}{\partial x} + \frac{\partial q_n^e}{\partial x} = Q_{ee} + Q_{ei}, \tag{6d}$$

$$n_i u_{ix} \frac{\partial T_{ix}}{\partial x} + 2 n_i T_{ix} \frac{\partial u_{ix}}{\partial x} + \frac{\partial q_n^i}{\partial x} = Q_{ii}, \tag{6e}$$

where x is the parallel direction coordinate. The electron inertia terms are neglected due to the small electron mass. The thermal force is written as $R = -\alpha n dT/dx$ with α the thermal force coefficient, $q_n^{e,i}$ are the parallel heat fluxes from the definition of Chew *et al*[23],

$$q_n \equiv \int m (v_x - u_x)^3 f d^3\mathbf{v}, \tag{7}$$

and $Q_{ee,ei}$ are the electron temperature isotropization terms due to electrons colliding with electrons and ions, respectively. In the intermediate collisional regime, these can be written as[24]

$$Q_{ee,ei} = 8 n_e \nu_{ee,ei} T_{ey} \frac{T_{ex}}{T_{ey} - T_{ex}} \Big[-3 + \Big(3\sqrt{\frac{T_{ex}}{T_{ey} - T_{ex}}} + \sqrt{\frac{T_{ey} - T_{ex}}{T_{ex}}} \Big) \arctan \sqrt{\frac{T_{ey} - T_{ex}}{T_{ex}}} \Big], \tag{8}$$

with the anisotropic plasma collision rate defined as[24]

$$\nu_{ee} = \frac{n_e}{n_i} \frac{\nu_{ei}}{Z\sqrt{2}} = \frac{\sqrt{\pi}}{2} n_e \frac{e^4}{(4\pi\varepsilon_0)^2} \frac{\ln\Lambda}{\sqrt{m_e T_{ex} T_{ey}}}, \tag{9}$$

and T_{ey} being the perpendicular temperature. The ion temperature isotropization due to collisions with ions and electrons are $Q_{ii,ie}$ respectively. In the collisional limit, these can be obtained from Eq. 8 by replacing the electron terms with the ion terms. Typically, Q_{ii} is not negligible due to the significant difference between T_{ix} and T_{iy}, while Q_{ie} is negligible due to the low ion-electron collision rate ν_{ie}. The set of equations is derived directly from taking moments of the Boltzmann equation without further assumptions. These equation are closed by evaluating the higher order moment (q_n) and collision terms from kinetic simulation results rather than simply assuming adiabatic indices γ_e and γ_i. Additionally, if the system is closed by dropping the heat flux and collisional energy exchange terms in the eneregy equations, then the indices $\gamma_{e,i} = 3$. The particle source is assumed to be far from the presheath region, so it is not included on the right-hand side of the transport equations.

B. Derivation of the transport-dependent Bohm speed

The Bohm speed can be obtained by inserting the plasma transport model into Eq. 5 for the electron and ion density gradients. Combining the electron continuity, momentum, and energy conservation equations by eliminating $\partial T_{ex}/\partial x$ and $\partial u_{ex}/\partial x$, we obtain, for spatially monotonic ϕ,

$$\frac{\partial n_e}{\partial \phi} = \frac{e n_e}{(3+2\alpha) T_{ex}} + \frac{1+\alpha}{(3+2\alpha) u_{ex} T_{ex}} \Big(\frac{\partial q_n^e}{\partial \phi} + \frac{Q_{ee} + Q_{ei}}{E} \Big), \tag{10}$$

where $E = -\partial\phi/\partial x$ is the electric field. For ions, the inertia term is included and similar analysis gives

$$\frac{\partial n_i}{\partial \phi} = \frac{1}{3 u_i T_{ix} - m_i u_{ix}^3} \left(\frac{\partial q_n^i}{\partial \phi} + \frac{Q_{ii}}{E} \right) - \frac{Z e n_i - \alpha n_e \partial T_{ex}/\partial\phi}{3 T_i - m_i u_{ix}^2}. \tag{11}$$

Substituting Eqs. 10 and 11 into Eq.5 gives the Bohm criterion that provides a lower bound for the ion flow speed

$$u_{ix}^{se} \geq u_{Bohm} \equiv \sqrt{(\beta T_{ex}^{se} + 3 T_{ix}^{se})/m_i}, \tag{12}$$

with the heat flux factor β

$$\beta \equiv \frac{3 - \frac{3+2\alpha}{Z e \Gamma_i^{se}} \left(\frac{\partial q_n^i}{\partial \phi} + \frac{Q_{ii}}{E} \right) + \frac{\alpha}{e\Gamma_e^{se}} \left(\frac{\partial q_n^e}{\partial \phi} + \frac{Q_{ee} + Q_{ei}}{E} \right)}{1 + \frac{1+\alpha}{e\Gamma_e^{se}} \left(\frac{\partial q_n^e}{\partial \phi} + \frac{Q_{ee} + Q_{ei}}{E} \right)}. \tag{13}$$

Here $\Gamma_{e,i} = n_{e,i} u_{ex,ix}$, is the flux and all quantities on the right-hand side of Eq. 13 with superscript *se* are evaluated locally at the sheath entrance, which can be interpreted here as the presheath-sheath transition region. Eqs.12 and 13 give the Bohm speed that accounts for the heat flux and the transport quantities for a plasma with varying collisionality. In the low collisionality limit, all the transport terms $\alpha, Q_{ee}, Q_{ei}, Q_{ii} \to 0$, and Eq.13 reduces to the collisionless presheath limit in Ref. 7. In the high collisionality regime, at first glance, the collisional isotropization terms, Q, seem to play a minor role in determining the Bohm speed since $T_y - T_x \approx 0$. Here, an estimation of Q can be conducted to show that it may not be negligible. Let $X = \sqrt{(T_{ey} - T_{ex})/T_{ex}}$ be the electron anisotropic coefficient. Expanding Q_{ee} near $X = 0$ by ignoring terms of higher-order than $O(X^2)$, we have

$$Q_{ee} = \frac{32}{15} n_e \nu_{ee} T_{ex} X^2. \tag{14}$$

The collisional temperature isotropization enters the Bohm speed with normalization by the product of electron particle flux and electric field at the sheath entrance,

$$\begin{aligned} \frac{Q_{ee} + Q_{ei}}{e\Gamma_e E} &\approx (1 + \sqrt{2}Z) \frac{32}{15} \frac{n_e \nu_{ee} T_{ey} X^2}{e n_e u_{ex} E} \\ &= (1 + \sqrt{2}Z) \frac{32}{15} \frac{v_{th,e}}{u_{ex}^{se}} \frac{\lambda_D}{\lambda_{mfp}} \frac{T_{ey}}{eE\lambda_D} X^2 \\ &\approx (1 + \sqrt{2}Z) \frac{32}{15} \sqrt{\frac{T_{ex}^{se}}{\beta T_{ex}^{se} + 3 T_{ix}^{se}}} \frac{\sqrt{m_i/m_e}}{K_n^{sh}} \frac{T_{ey}}{\lambda_D e E} X^2. \end{aligned} \tag{15}$$

In the collisionless limit, where $K_n^{sh} \to \infty$ while other terms on the right-hand side of Eq.15 are bounded, $(Q_{ee}+Q_{ei})/e\Gamma_e E \to 0$. In the intermediate collisionality regime, where $K_n^{sh} \sim O(\sqrt{m_i/m_e})$, the larger temperature anisotropy and the smaller local electric field produce a $(Q_{ee}+Q_{ei})/e\Gamma_e E \sim O(1)$. For highly collisional plasmas, though the plasma is quite isotropic, the large ratio of $\sqrt{m_i/m_e}/K_n^{sh}$ makes $(Q_{ee}+Q_{ei})/e\Gamma_e E \sim O(1)$. A similar analysis can be performed for ions and one finds that $Q_{ii}/(e\Gamma_e E)$ is K_n^{sh} small but non-negligible since ions are more anisotropic than electrons.

III. VPIC KINETIC SIMULATION OF PRESHEATH-SHEATH TRANSITION WITH AN UPSTREAM VOLUMETRIC SOURCE

A. Simulation setup

To verify the predictive model of the Bohm speed in Eq. 12 and Eq. 13, and illustrate the importance of transport physics on the presheath-sheath transition, kinetic simulations are performed using VPIC[20] for a slab plasma bounded by absorbing walls. Initially, a hydrogen plasma ($Z=1$) is magnetized with a magnetic field perpendicular to the wall to suppress the Weibel instability[17]. The plasma with temperature $T_e = T_i = T_0$ is uniformly distributed in the domain. To balance the particle loss at the walls, a uniform Maxwellian source with temperature T_0 is injected into the plasma in the middle of the domain ($S \in [3L/8, 5L/8]$), mimicking the upstream source of a scrape-off layer in a tokamak. The source injection rate is set to be equal to the ion loss rate at the wall such that a fast equilibrium can be reached. Initially, since the plasma is uniform and isotropic, the collisionality of the system is characterized by a nominal K_n defined as the ratio of the initial electron mean free path to the initial Debye length. To elucidate the role of transport physics in setting the Bohm speed, the simulations cover a wide range of collisionality with nominal $K_n \in [20, 5000]$,corresponding to different combinations of initial density and temperature, as shown in Fig. 1. ~~Note that here the nominal K_n is calculated using the isotropic electron-ion Coulomb frequency, corresponding to different combinations of density and temperature, as shown in Fig. 1~~. The Coulomb collision is implemented using Takizuka and Abe's model[27] in the VPIC simulations.In the absence of net current, the thermal force and the temperature isotropization terms can be evaluated directly from the collision integral

$$R_T = \int m_e v_x \left(\frac{\partial f}{\partial t}\right)_{coll}^{ei} d^3v, \tag{16a}$$

$$Q_{sr} = \int m_s (v_x - u_x)(v_x - u_x) \left(\frac{\partial f}{\partial t}\right)_{coll}^{sr} d^3v, \tag{16b}$$

where s and r denote the interacting species and $(\partial f/\partial t)_{coll}$ is the rate of change of the distribution function due to the Coulomb collisions.~~which can be evaluated using Takizuka and Abe's model[27] in the VPIC simulations.~~ More detailed simulation parameters are listed in Table. I.

TABLE I: Simulation parameters for a collisional presheath

System length	$L = 256\lambda_D$
Number of super-particles per cell	10000
Mass ratio	$m_i/m_e = 1836$
Collisionality	$K_n \in [20, 5000]$
Source particle injection rate	$R_{inj} = R_{Ion\ loss}$
Plasma source region	$S \in [3L/8, 5L/8]$

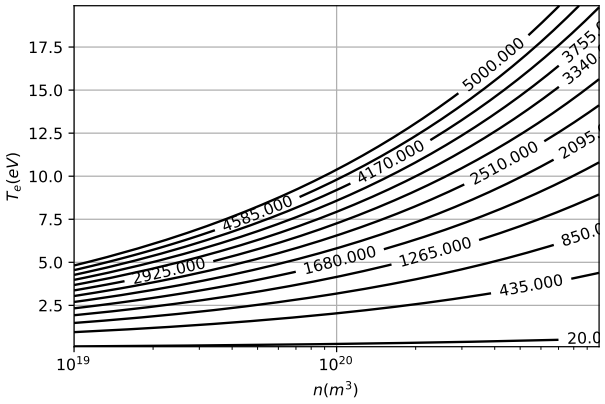

FIG. 1: The nominal K_n as a function of the density n and electron temperature T_e.

B. Plasma profile at steady state

In Fig.2 we show the steady-state plasma profiles for $K_n = 50$. Since the system is symmetric, we only show results of one side of the domain without the source region ($0-80\lambda_D$). The density and temperature of both species are normalized to their initial values n_0 and T_0, the potential ϕ to T_0/e, the ion flow to the local adiabatic sound speed $c_s = \sqrt{(T_{ex}+3T_{ix})/m_i}$. It clearly illustrates that, away from the asymptotic limit $\lambda_D/L \to 0$, a transition region, rather than a sharp boundary, exists between the presheath and the sheath. In this region, the quasineutrality is weakly violated, and the plasma flow and potential gradient increase gradually towards the sheath. The electron temperature is anisotropic within the Knudsen layer (from the wall to $x \sim \lambda_{mfp}$) due to decompressional cooling in the $x-$direction for a collisionless case[17]. T_{ey} is significantly increased near the material surface due to the finite heat flux of $q_{es} \equiv \int m(v_y-u_y)^2(v_x-u_x) f d^3\mathbf{v}$ corresponding to T_{ey}, which has a negative gradient in the sheath region next to the left wall. Further upstream, the intense Coulomb collision in the presheath region can eliminate the electron temperature anisotropy. However, strong ion temperature anisotropy exists over the whole domain due to the slow ion-electron and ion-

ion collision rates. The plasma temperature gradient exists in the presheath and sheath region in a steady-state plasma. Despite the large electron thermal conductivity, the isothermal electron assumption in the sheath model may not be valid, indicating more involved transport physics need to be considered in the presheath-sheath transition problem.

IV. DETERMINATION OF SHEATH TRANSITION REGION FROM SIMULATION DATA AND LOCAL BOHM SPEED

A. Sheath entrance versus sheath transition region

The definition of the sheath entrance in the asymptotic limit[6,8] of $\lambda_D/L \to 0$ is not applicable to simulations or real situations where the sheath has finite thickness and the breakdown of quasineutrality is not abrupt. The plasma density and potential profile (Fig. 2a and 2b) show there exists a transition region that smoothly joins the quasineutral plasma and the non-neutral sheath together. In this transition region, the quasineutrality is preserved to the zeroth order $n_e \approx Zn_i$, while the net charge density gradient begins to dominate in the linearized Poisson equation and the quasineutrality is perturbed to the first order or weakly perturbed. The definition of weakly-perturbed-quasineutrality is consistent with the Bohm criterion (Eq. 5). This means that in real situations the sheath entrance becomes a sheath transition region as opposed to a single point in the asymptotic limit, and that Bohm speed should vary inside this transition region. Away from the asymptotic limit, the Bohm (sheath) criterion in Eq. 5 should be applied in the transition region where quasineutrality is weakly perturbed. To determine a point for the nominal sheath entrance, a location may be chosen at the edge of the transition layer that connects the non-neutral sheath and the weakly non-neutral transition layer. In Ref. 6, it is suggested that this point can be located where the charge separation level $\overline{\rho} = |(n_i - n_e)/n_i|$ is smaller than some threshold. The choice of this threshold is somewhat arbitrary since the breakdown of quasineutrality is not abrupt in a physical sheath. $\overline{\rho}$ is assumed to be 1% or 10% for some cases[6,7]. However, a small $\overline{\rho}$ does not always guarantee the accuracy of the Bohm criterion, since $\overline{\partial\rho/\partial x}$ may be large. Here, $\overline{\partial\rho/\partial x}$ is the fractional charge density gradient

$$\overline{\frac{\partial\rho}{\partial x}} = \left|\frac{\partial n_e}{\partial x} - \frac{\partial n_i}{\partial x}\right| / |\frac{\partial n_e}{\partial x} + \frac{\partial n_i}{\partial x}|. \tag{17}$$

In Fig. 3, the time-averaged results of $\overline{\rho}$ is compared with $\overline{\partial\rho/\partial x}$ for a case with $K_n = 50$. In this case, a 10% breakdown of quasineutrality (at about $2.0\lambda_D$) produces $\overline{\partial\rho/\partial x}$ of 50%, and a 1% breakdown of quasineutrality (at about $4.0\lambda_D$) produces $\overline{\partial\rho/\partial x}$ of 20%. In both situations, the Bohm criterion in Eq. 5 is no longer accurate.

From the definition of the weakly-perturbed quasineutrality, it is more natural to identify the sheath transition region using the fractional charge density gradient $\overline{\partial\rho/\partial x}$ rather than $\overline{\rho}$. It should not be too small to avoid reaching the quasineutral presheath region, nor too big for the accuracy of the model. The sheath entrance can be defined as the edge of the transition region and is arbitrarily chosen at the point where $\overline{\partial\rho/\partial x}$ is roughly 10%, such that Eq. 5 barely applies. For $K_n = 50$ in Fig. 3, the nominal sheath entrance can be placed at $5.0\lambda_D$ for $\overline{\partial\rho/\partial x}$ being 10%. Note that in the sheath region, Eq. 5 is valid only for the greater sign and the zeroth-order term in the net charge expansion dominates. Though Eq. 5 holds in the quasineutral region, it is not meaningful since Poisson's equation is not used to solve the potential. In the sheath transition region, the first-order term $\partial n_e/\partial x - \partial n_i/\partial x$ in the net charge expansion begins to dominate, and Eq. 5 applies with the equal sign without significant error.

The plasma at the sheath entrance can be characterized by several dimensionless parameters: the temperature ratios T^{se}_{ey}/T^{se}_{ex}, T^{se}_{iy}/T^{se}_{ix}, the normalized electric field $eE^{se}\lambda_D/T^{se}_{ex}$, and the local sheath Knudsen number K^{se}_n. The position of the sheath entrance x_{se} is identified where the fractional charge density gradient is 10%. All these normalized parameters are presented in Table. II. The location of the sheath entrance oscillates around $x = 5 - 5.5\lambda_D$ and does not depend on the collisionality in any significant way. As expected, the electron and ion temperatures become increasingly anisotropic as K_n increases. The ions are more anisotropic than the electrons due to the slow ion-ion collisions. The normalized local electric field decreases with increasing collisionality, making $(Q_{ee} + Q_{ei})/e\Gamma_e E \sim O(1)$ in the evaluation of the Bohm speed.

TABLE II: Normalized parameters at the sheath entrance

K_n	K^{se}_n	$\frac{T^{se}_{ey}}{T^{se}_{ex}}$	$\frac{T^{se}_{iy}}{T^{se}_{ix}}$	$\frac{eE^{se}\lambda_d}{T^{se}_{ex}}$	$\frac{x_{se}}{\lambda_D}$
20	5.26	1.01	1.12	-0.044	5.0
50	13.13	1.05	1.32	-0.032	5.0
200	50.04	1.09	2.21	-0.019	5.5
500	116.6	1.13	3.20	-0.017	5.5
1000	220.4	1.19	4.03	-0.016	5.5
2000	420.9	1.29	4.66	-0.015	5.5
5000	1932	1.60	5.35	-0.014	5.0

B. Local Bohm speed over the sheath transition region

The Bohm speed evaluation model can be applied to the sheath transition layer that includes the nominal sheath entrance discussed in the previous section. All the physical quantities in Eq. 12 and Eq. 13 can be obtained from the simulation to evaluate the Bohm speed. After the simulation reaches steady-state, a time-averaging of the physical parameters over 200000 timesteps is employed to reduce the PIC noise. In Fig. 4, we compare the ion exit flow speed with the calculated Bohm speed as a function of the distance from the wall for two test cases with different collisionality ($K_n = 50$ and $K_n = 500$). In the non-neutral sheath region near the wall, the ion exit flow speed diverges from the model prediction

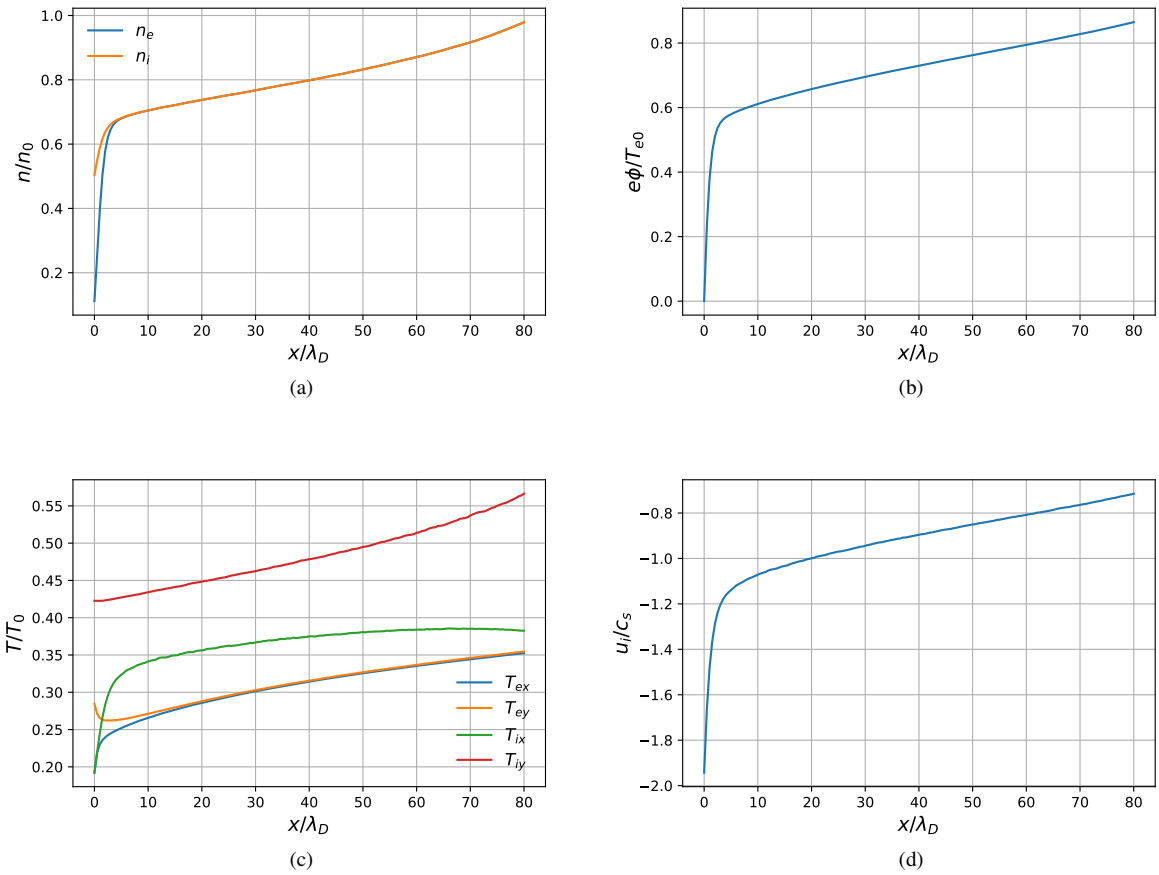

FIG. 2: Steady-state plasma profiles for a collisional presheath ($K_n = 50$) (a) Density of electron and ion normalized by the initial density n_0; (b) Potential profile normalized by T_e/e; (c) Temperature of electron and ion in x and y direction, normalized by the initial temperature T_0; (d) Ion velocity normalized by the adiabatic sound speed $c_s = \sqrt{(T_{ex} + 3T_{ix})/m_i}$.

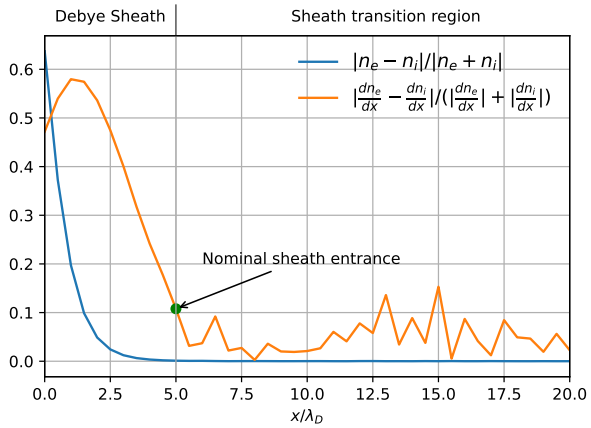

FIG. 3: Normalized net charge density $\overline{\rho}$, charge density gradient $\overline{\partial\rho/\partial x}$ for $K_n = 50$.

of Bohm speed, as expected. Further upstream, in the sheath transition region, the local Bohm speed matches the ion exit flow despite the PIC noise. The breakdown of u_{Bohm} from Eq. 12 and Eq. 13 is an accurate indication of transitioning into the non-neutral Debye sheath.

V. ROLES OF DIFFERENT TRANSPORT PHYSICS IN SETTING THE BOHM SPEED

To elucidate the role of transport physics in the presheath-sheath transition problem, both sides of the electron momentum and energy transport equations are plotted in Fig. 5a and 5b for a case with collisional presheath ($K_n = 50$). The momentum and energy transport of the system reaches a steady-state by comparing the orange and blues line in Fig. 5a and 5b. The thermal force term R_T matches the sum of the other terms and agrees with the theoretical limit $-0.71 n_e dT/dx$ in the collisional presheath region[22]. Within the Knudsen layer, however, the plasma can be considered as collisionless and R_T deviates from $-0.71 n_e dT/dx$. By comparing the orange and green curves in Fig. 5b, it is clear that the temperature isotropization terms Q_{ee} and Q_{ei} make a difference within the

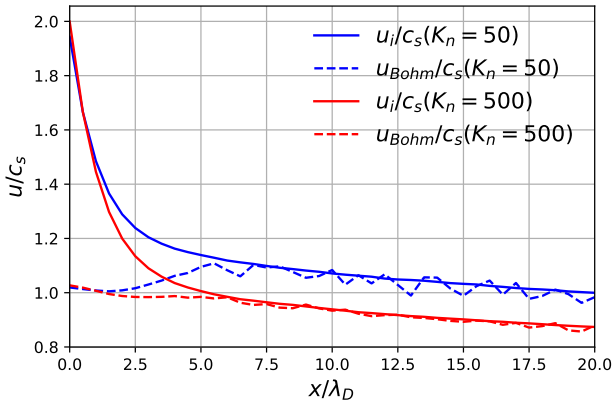

FIG. 4: Ion exit flow speed and Bohm speed calculated from Eq. (12,13) normalized by the adiabatic sound speed $c_s(\gamma_e = 1, \gamma_i = 3)$ over distance from the wall for $K_n = 50$ and $K_n = 500$.

TABLE III: Normalized parameters at the sheath entrance where the fractional charge density gradient is 10% and the Bohm speed calculated from Eq. 12 and Eq. 13. The cases for $K_n = 20, 200, 5000$ are from Ref. 26.

K_n	$\frac{u_{ix}}{c_s}$	$\frac{u_{Bohm}}{c_s}$	$\frac{1}{e\Gamma_e^{se}}\frac{\partial q_n^e}{\partial \phi}$	$\frac{Q_{ee}^{se}+Q_{ei}^{se}}{e\Gamma_e^{se}E^{se}}$	$\frac{1}{e\Gamma_i^{se}}\frac{\partial q_n^i}{\partial \phi}$	$\frac{Q_{ii}^{se}}{e\Gamma_i^{se}E^{se}}$	α^{se}
20	1.25	1.20	-1.63	1.48	-0.05	0.18	0.59
50	1.14	1.10	-3.27	3.59	-0.20	0.26	0.51
200	1.02	1.00	-2.20	3.55	-0.22	0.38	0.45
500	0.99	0.98	-0.68	2.29	-0.08	0.32	0.39
1000	0.98	0.96	-0.18	1.69	0.14	0.23	0.18
2000	0.95	0.94	0.44	1.36	0.36	0.12	0.11
5000	0.94	0.93	0.23	1.17	0.52	0.07	0.04

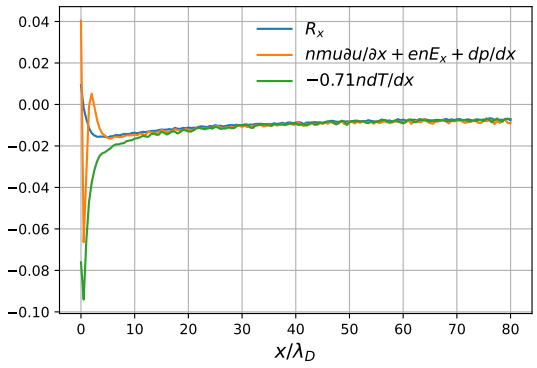

(a)

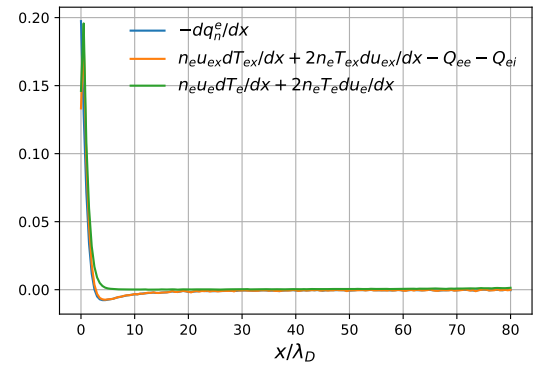

(b)

FIG. 5: Terms in the electron energy and momentum transport equations for a collisional presheath case($K_n = 50$). (a) Different terms in the electron momentum equation and the analytical thermal force $R_T = -0.71 n_e dT_{ex}/dx$; (b) Different terms in the electron energy equation.

Knudsen layer, where the electron temperature is anisotropic. Thus, the transport physics enters the presheath-sheath transition problem through the thermal force R_T and the temperature isotropization $Q_{ee,ei}$ and Q_{ii} terms and will affect the evaluation of the Bohm speed.

The collisionality of the system can affect the transport physics and thus influence the Bohm speed. For plasmas in different collisional regimes ($K_n \in [20, 5000]$), the transport terms in Eq. 13 are calculated from the simulation data and shown in Table. III. The calculated Bohm speed from Eq. 12 and 13 is contrasted with the ion flow speed, and both are normalized with the local adiabatic sound speed $c_s = \sqrt{(T_{ex} + 3T_{ix})/m_i}$. All the parameters in Tab. III are locally evaluated at the nominal sheath entrance, which is identified where the fractional charge density gradient is 10%.

Overall, the expression of the Bohm speed is accurate over a range of collisionality, as can be seen by comparing the second and third columns of Table. III. The electron heat flux and temperature isotropization terms play the most critical role in determining the Bohm speed. The normalized electron flux gradient $(\partial q_n^e/\partial\phi)/(e\Gamma_e)$ is naturally the dominant term at small length scales. The Coulomb collision changes the energy transport such that the electron heat flux profile changes with K_n, as shown in Fig. 6. The normalized electron isotropization term $(Q_{ee} + Q_{ei})/(e\Gamma_e^{se}E^{se}) \sim O(1)$ from the simulation result, in accordance with the scale analysis in Eq. 15. It is of similar order as the normalized electron heat flux gradient in impacting the Bohm speed. Note that for low collisionality plasmas, the normalized electron isotropization term is not negligible due to the large electron temperature anisotropization as well as the smallness of the normalized electric field $eE^{se}\lambda_D/T_{ex}^{se}$ (See Table. II). Despite the large ion to electron mass ratio in a hydrogen plasma, the ion heat flux and temperature isotropization make a small but non-negligible contribution to the Bohm speed. Finally, the thermal force coefficient α^{se} decreases for increasing K_n and is smaller than the Braginskii value as expected.

Another way of quantifying the importance of individual transport physics terms in the Bohm speed is to calculate a "modified Bohm speed" by setting different terms to zero in Eq. 12 and Eq. 13. The results are shown and compared in

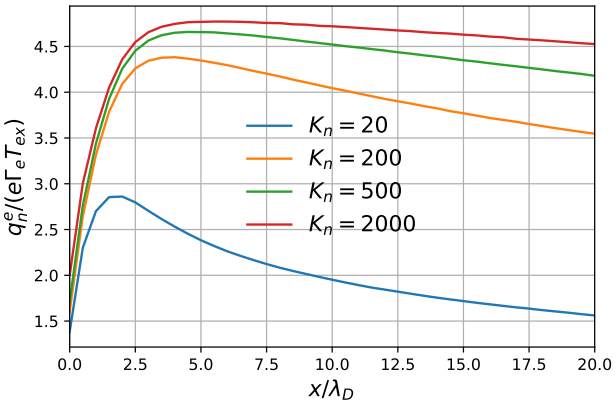

FIG. 6: Normalized electron heat flux as a function of the position for different collisionality.

Table. IV.

TABLE IV: The influence of different terms in Eq. 12 and Eq. 13 on the Bohm speed

K_n	$\frac{u_{ix}}{c_s}$	$\frac{u_{Bohm}}{c_s}$	$\alpha = 0$	$\frac{\partial q_n^i}{\partial \phi}, Q_{ii} = 0$	$Q_{ee,ei} = 0$	$\frac{\partial q_n^e}{\partial \phi} = 0$
20	1.25	1.20	1.20	1.26	0.77	1.00
50	1.14	1.10	1.11	1.11	0.86	0.97
200	1.02	1.00	1.01	1.03	0.79	0.96
500	0.99	0.98	0.98	1.01	3.05	0.96
1000	0.98	0.96	0.97	1.02	1.15	0.96
2000	0.95	0.94	0.94	1.01	1.03	0.94
5000	0.94	0.93	0.92	1.02	1.00	0.92

As is shown in Table.IV, the thermal force coefficient α^{se} has a negligible influence on the Bohm speed. The ion heat flux and temperature isotropization terms can affect the result slightly for highly collisional cases. They have an increasing influence on the Bohm speed as the collisionality decreases because the normalized ion and electron heat flux derivatives are comparable for low collisionality cases ($K_n = 2000, 5000$) in Table. IV. The normalized electron heat flux, on the other hand, has a decreasing effect on the calculation of the Bohm speed as the collisionality decreases. The electron temperature isotropization $Q_{ee,ei}$ play a crucial role in determining the Bohm speed. Especially for the case where $K_n = 500$, the Bohm speed estimation is poor with $Q_{ee,ei} = 0$ since the denominator of Eq. 13 is close to zero when $Q_{ee,ei}$ is ignored. The accuracy of the Bohm speed calculation is most significantly affected by the electron temperature isotropization term.

From Fig. 4, one can see that the model captures the varying Bohm speed in the transition region with reasonable accuracy. Here, the transport terms are plotted in Fig. 7 for $K_n = 50$ to show their variation in the sheath transition region. Notice that the collisionality inside the transition layer (or the local Knudsen number K_n^{se}) varies, as do the transport terms. As we can see, although all the normalized physical quantities, in particlar the electron heat flux derivative and the electron collisional isotropization terms, vary over the transition region, these variations can compensate with each other such that Eq. 12 and Eq. 13 predict the Bohm speed accurately as shown in Fig. 4.

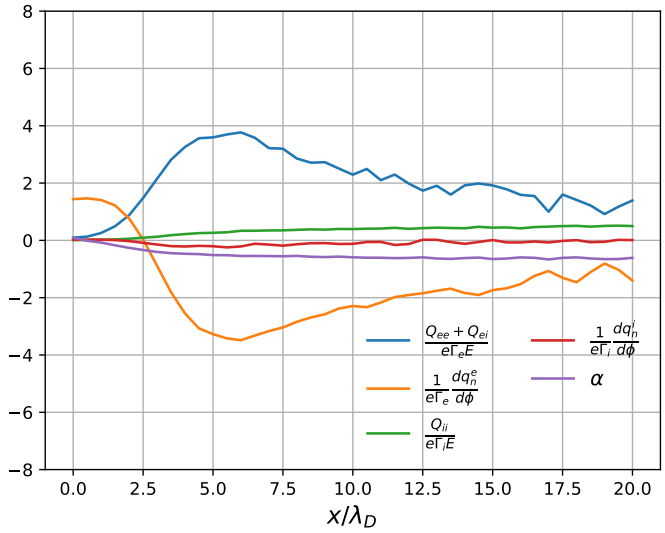

FIG. 7: Normalized parameters determining the Bohm speed in the sheath transition region for $K_n = 50$.

A. COMPARISON OF TEMPERATURE ISOTROPIZATION TERMS FROM KINETIC SIMULATION TO CHODURA'S CLOSURE

For all the Bohm speed calculations presented here, the terms with respect to collisions, namely the thermal force R_T and the collisional isotropization $Q_{ei,ee,ii}$, are directly evaluated from the Coulomb collision operator in the simulation using Eq. 16. The thermal force R_T deviates from Braginskii's theory, especially for the low collisionality cases (see Table.III). In the high collisionality limit, Chodura and Pohl provide a closure for the anisotropic plasma transport (Eq. 8). Here, $Q_{ee,ei}$ from both the simulations and Chodura's evaluations for cases with different collisionality ($K_n = 50, 200$) are shown in Fig. 8. It demonstrates that the Chodura's closure captures the underlying isotropization physics with reasonable accuracy for high collisionality plasmas. As the collisionality decreases, the deviation is significant. A kinetic correction is needed for evaluation of the Bohm speed in Eq. 12 and Eq. 13 over the sheath transition region.

VI. CONCLUSIONS

In the classical sheath model, adiabatic indices for electrons and ions are assumed to close the system, and a Bohm speed is obtained at the sheath entrance in the asymptotic limit

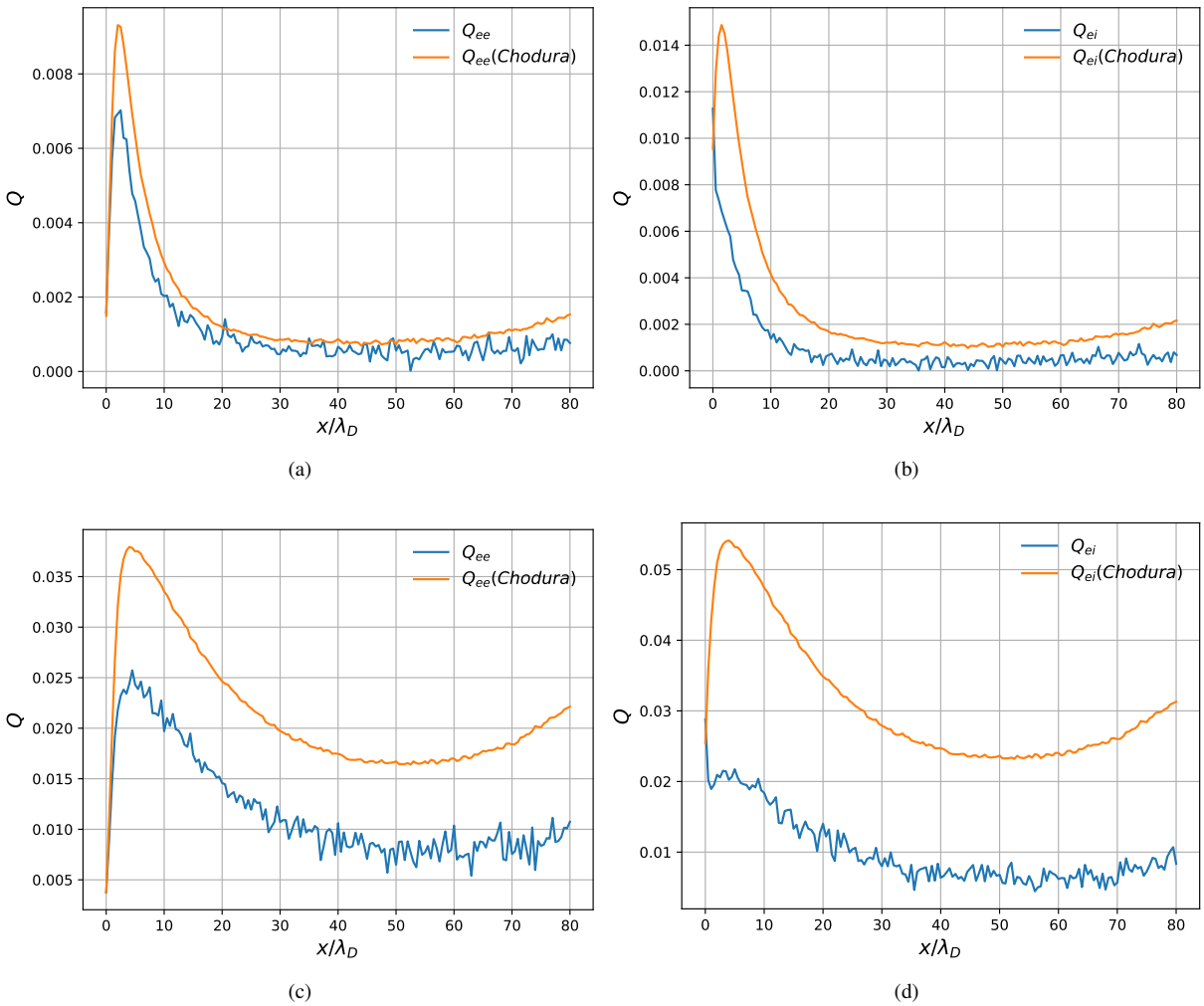

FIG. 8: Comparison of the Q_{ee} and Q_{ei} terms evaluated from the kinetic simulation with those calculated by Eq. 8 for (a,b) $K_n = 50$ and (c,d) $K_n = 200$ cases.

$\lambda_D/L \to 0$. Here, an expression for the Bohm speed away from the asymptotic limit is derived from a set of anisotropic plasma transport equations, where transport physics including the heat flux, temperature isotropization, and thermal force are considered. Away from the asymptotic limit, the sheath entrance is extended to a sheath transition region, where the quasineutrality is weakly perturbed. The sheath transition region is identified using the fractional charge density gradient, since it is a more sensitive measure of the Bohm criterion than the net charge separation level. By performing the first-principle kinetic simulations using VPIC, it is shown that Eq. 12 and Eq. 13 can predict the Bohm speed accurately in the sheath transition layer over a range of collisionality. Further analysis shows that the electron heat flux and the electron temperature isotropization have a significant influence in determining the Bohm speed, while the thermal force and the ion isotropization are not negligible but unimportant. The Bohm criterion analysis presented here can be readily extended to plasmas where more complex transport is involved and the resulting Bohm speed will be consistent with the underlying transport model. The plasma-sheath transition problem is kinetic and the Chodura and Pohl's closure for $Q_{ee,ei,ii}$, as well as Braginskii's closure for the thermal force R_T, which are derived in high collisionality limit, are not adequate to close the system.

ACKNOWLEDGMENTS

We thank the U.S. Department of Energy Office of Fusion Energy Sciences and Office of Advanced Scientific Computing Research for support under the Tokamak Disruption Simulation (TDS) Scientific Discovery through Advanced Computing (SciDAC) project at both Virginia Tech under grant number DE-SC0018276 and Los Alamos National Laboratory (LANL) under contract No. 89233218CNA000001. Yanzeng Zhang was supported under a Director's Postdoctoral Fellowship at LANL. This research used resources of the National

Energy Research Scientific Computing Center (NERSC), a U.S. Department of Energy Office of Science User Facility operated under Contract No.DE-AC02-05CH11231. Useful discussions with Jun Li are acknowledged.

[1] K.-U. Riemann, "The bohm criterion and sheath formation," Journal of Physics D: Applied Physics **24**, 493–518 (1991).

[2] V. Rozhansky, E. Kaveeva, P. Molchanov, I. Veselova, S. Voskoboynikov, D. Coster, G. Counsell, A. Kirk, S. Lisgo, and and, "New b2solps5.2 transport code for h-mode regimes in tokamaks," Nuclear Fusion **49**, 025007 (2009).

[3] F. Halpern, P. Ricci, S. Jolliet, J. Loizu, J. Morales, A. Mosetto, F. Musil, F. Riva, T. Tran, and C. Wersal, "The gbs code for tokamak scrape-off layer simulations," Journal of Computational Physics **315**, 388–408 (2016).

[4] R. Schneider, X. Bonnin, K. Borrass, D. P. Coster, H. Kastelewicz, D. Reiter, V. A. Rozhansky, and B. J. Braams, "Plasma edge physics with b2-eirene," Contributions to Plasma Physics **46**, 3–191 (2006), https://onlinelibrary.wiley.com/doi/pdf/10.1002/ctpp.200610001.

[5] D. BOHM, "The characteristics of electrical discharges in magnetic fields," Qualitative Description of the Arc Plasma in a Magnetic Field (1949).

[6] S. D. Baalrud, B. Scheiner, B. Yee, M. Hopkins, and E. Barnat, "Extensions and applications of the bohm criterion," Plasma Physics and Controlled Fusion **57**, 044003 (2015).

[7] X.-Z. Tang and Z. Guo, "Critical role of electron heat flux on bohm criterion," Physics of Plasmas **23**, 120701 (2016), https://doi.org/10.1063/1.4971808.

[8] L. Tonks and I. Langmuir, "A general theory of the plasma of an arc," Phys. Rev. **34**, 876–922 (1929).

[9] K.-U. Riemann, "The bohm criterion and boundary conditions for a multicomponent system," IEEE Transactions on Plasma Science **23**, 709–716 (1995).

[10] X.-Z. Tang and Z. Guo, "Kinetic model for the collisionless sheath of a collisional plasma," Physics of Plasmas **23**, 083503 (2016), https://doi.org/10.1063/1.4960321.

[11] P. C. Stangeby, *The Plasma Boundary of Magnetic Fusion Devices* (Taylor & Francis, 2000).

[12] X.-Z. Tang and Z. Guo, "Sheath energy transmission in a collisional plasma with collisionless sheath," Physics of Plasmas **22**, 100703 (2015), http://dx.doi.org/10.1063/1.4933415.

[13] S. A. Self and H. N. Ewald, "Static theory of a discharge column at intermediate pressures," The Physics of Fluids **9**, 2486–2492 (1966).

[14] R. C. Bissell, P. C. Johnson, and P. C. Stangeby, "A review of models for collisionless one-dimensional plasma flow to a boundary," Physics of Fluids B: Plasma Physics **1**, 1133–1140 (1989).

[15] P. Cagas, A. Hakim, J. Juno, and B. Srinivasan, "Continuum kinetic and multi-fluid simulations of classical sheaths," Physics of Plasmas **24**, 022118 (2017), https://doi.org/10.1063/1.4976544.

[16] P. Cagas, A. H. Hakim, and B. Srinivasan, "A boundary value "reservoir problem" and boundary conditions for multi-moment multi-fluid simulations of sheaths," Physics of Plasmas **28**, 014501 (2021), https://doi.org/10.1063/5.0024510.

[17] X. Z. Tang, "Kinetic magnetic dynamo in a sheath-limited high-temperature and low-density plasma," Plasma Physics and Controlled Fusion **53**, 082002 (2011).

[18] R. N. Franklin and J. R. Ockendon, "Asymptotic matching of plasma and sheath in an active low pressure discharge," Journal of Plasma Physics **4**, 371–385 (1970).

[19] R. N. Franklin, "Whereisthe sheath edge ?" Journal of Physics D: Applied Physics **37**, 1342–1345 (2004).

[20] B. B. K.J. Bowers, B.J. Albright and T. Kwan, "Ultrahigh performance three-dimensional electromagnetic relativistic kinetic plasma simulation," Phys. Plasmas . **10:1**, 183 (2008).

[21] K.-U. Riemann, "The influence of collisions on the plasma sheath transition," Physics of Plasmas **4**, 4158–4166 (1997), https://doi.org/10.1063/1.872536.

[22] S. I. Braginskii, "Transport Processes in a Plasma," Reviews of Plasma Physics **1**, 205 (1965).

[23] G. F. Chew, M. L. Goldberger, F. E. Low, and S. Chandrasekhar, "The boltzmann equation an d the one-fluid hydromagnetic equations in the absence of particle collisions," Proceedings of the Royal Society of London. Series A. Mathematical and Physical Sciences **236**, 112–118 (1956), https://royalsocietypublishing.org/doi/pdf/10.1098/rspa.1956.0116.

[24] R. Chodura and F. Pohl, "Hydrodynamic equations for anisotropic plasmas in magnetic fields. II. transport equations including collisions," Plasma Physics **13**, 645–658 (1971).

[25] Z. Guo and X.-Z. Tang, "Parallel transport of long mean-free-path plasmas along open magnetic field lines: Plasma profile variation," Physics of Plasmas **19**, 082310 (2012), http://dx.doi.org/10.1063/1.4747167.

[26] Y. Li, B. Srinivasan, Y. Zhang, and X.-Z. Tang, "Bohm criterion of plasma sheaths away from asymptotic limits," Phys. Rev. Lett. **128**, 085002 (2022).

[27] T. Takizuka and H. Abe, "A binary collision model for plasma simulation with a particle code," Journal of Computational Physics **25**, 205 – 219 (1977).